LEVEL II 2 (2)

SECURITY CLASSIFICATION OF THIS PAGE (When Data Entered)

REPORT DOCUMENTATION PAGE

READ INSTRUCTIONS BEFORE COMPLETING FORM

1. REPORT NUMBER	2. GOVT ACCESSION NO. / 3. RECIPIENT'S CATALOG NUMBER
4. TITLE (and Subtitle): ULTRAVIOLET LASING TRANSITIONS IN DIATOMIC MOLECULES	5. TYPE OF REPORT & PERIOD COVERED: INTERIM PROGRESS REPORT
	6. PERFORMING ORG. REPORT NUMBER
7. AUTHOR(s): Joel Tellinghuisen	8. CONTRACT OR GRANT NUMBER(s): N00014-76-C-0450
9. PERFORMING ORGANIZATION NAME AND ADDRESS: Joel Tellinghuisen, Department of Chemistry, Vanderbilt University, Nashville, Tennessee 37235	10. PROGRAM ELEMENT, PROJECT, TASK AREA & WORK UNIT NUMBERS: DARPA Order No. 2840/10, Program Code 8E20
11. CONTROLLING OFFICE NAME AND ADDRESS: Defense Advanced Research Projects Agency, 1400 Wilson Boulevard, Arlington, Virginia 22209	12. REPORT DATE: July, 1978
	13. NUMBER OF PAGES: 20
14. MONITORING AGENCY NAME & ADDRESS (if different from Controlling Office): Physics Program, Physical Sciences Division, Office of Naval Research, 800 N. Quincy Street, Arlington, VA 22217	15. SECURITY CLASS. (of this report): Unclassified
	15a. DECLASSIFICATION/DOWNGRADING SCHEDULE

16. DISTRIBUTION STATEMENT (of this Report)

Approved for public release; distribution unlimited.

17. DISTRIBUTION STATEMENT (of the abstract entered in Block 20, if different from Report)

18. SUPPLEMENTARY NOTES

19. KEY WORDS (Continue on reverse side if necessary and identify by block number)

UV lasers, rare gas halide spectroscopy, halogen spectroscopy, Franck-Condon factors, vibrational relaxation

20. ABSTRACT (Continue on reverse side if necessary and identify by block number)

The work performed under this contract is primarily directed toward a better spectroscopic understanding of UV laser transitions in selected diatomic molecules. Specifically the work emphasizes the analysis of spectroscopic data for discrete (bound-bound) and diffuse (bound-free) transitions in the rare gas monohalide (AX) molecules, and discrete transitions in the homonuclear halogens. The primary aims of the work are (1) a specific, detailed identification of the laser transitions, including a description of the

electronic, and (for discrete systems) vibrational and rotational states involved in the transitions; (2) determination of potential curves for relevant electronic states; (3) calculation of intensity factors -- Franck-Condon factors and R-centroids for discrete systems, Franck-Condon densities and stimulated emission cross sections for diffuse systems; (4) evaluation of vibrational relaxation rates in the excited states from the pressure dependence of the emission spectrum; and (5) in some cases (XeF, I_2^*, Br_2^*) a determination of the kinetics of production and removal of the lower or terminal state of the laser transition. These studies are of relevance to the better understanding of these new lasers and to the development of more complete and correct mathematical models for describing and predicting their performance.

(6) ULTRAVIOLET LASING TRANSITIONS IN DIATOMIC MOLECULES.

(9) Interim Progress Report.

(11) (July [redacted] 78)

(12) 23p.

(15) Contract No. N00014-76-C-0450, // DARPA Order-2840
DARPA Order No. 2840/10
Program Code 8E20

(10) Joel Tellinghuisen, Principal Investigator
Department of Chemistry
Vanderbilt University
Nashville, Tennessee 37235
615/322-4873

The views and conclusions contained in this document are those of the author and should not be interpreted as necessarily representing the official policies, either expressed or implied, of the Defense Advanced Research Projects Agency or the U. S. Government.

INTERIM PROGRESS REPORT

(Contract No. N00014-76-C-0450)

ULTRAVIOLET LASTING TRANSITIONS IN DIATOMIC MOLECULES

I. Summary

The work performed under this contract is primarily directed toward a better spectroscopic understanding of UV laser transitions in selected diatomic molecules. Specifically the work emphasizes the analysis of spectroscopic data for discrete (bound-bound) and diffuse (bound-free) transitions in the rare gas monohalide (AX) molecules, and discrete transitions in the homonuclear halogens. The primary aims of the work are (1) a specific, detailed identification of the laser transitions, including a description of the electronic, and (for discrete systems) vibrational and rotational states involved in the transitions; (2) determination of potential curves for relevant electronic states; (3) calculation of intensity factors -- Franck-Condon factors and R-centroids for discrete systems, Franck-Condon densities and stimulated emission cross sections for diffuse systems; (4) evaluation of vibrational relaxation rates in the excited states from the pressure dependence of the emission spectrum; and (5) in some cases (XeF, I_2, Br_2) a determination of the kinetics of production and removal of the lower or terminal state of the laser transition. These studies are of relevance to the better understanding of these new lasers and to the development of more complete and correct mathematical models for describing and predicting their performance.

II. Accomplishments

A. Rare Gas Halide Studies

The outstanding achievement of this reporting period has been the preparation, submission, and publication of two lengthy papers on the XeF emission

spectrum. These works (listed below in Section IV), which have just appeared in print, provide the first detailed analysis of the B↦X laser transition in XeF (~3500 Å). They include a partial rotational analysis with approximate identification of the rovibrational levels which lase. Results of this analysis are now being corroborated in a followup study of the emission spectrum of a single isotopic species, $^{136}Xe^{19}F$. Good spectra for the latter have been obtained and the analysis is now in progress. At this stage one band (0-2) has been assigned and processed, giving results in good agreement with the just published values (which were somewhat speculative, as they were based on a rotational analysis of a single band, the 1-2 band). Ultimately the current work should provide a complete rotational and vibrational description of the X, B, and D states of XeF, and, from analysis of perturbations and splitting constants, an approximate determination of the C state.

In closely related work we have just completed and submitted a manuscript on the B↦X and D↦X systems of $^{136}Xe^{35}Cl$ -- the only AX molecule apart from XeF to display discrete structure in its spectrum. By using single isotopes of Xe and Cl, we have been able to greatly improve and expand on our previous vibrational analysis of the B↦X (laser) system in this molecule, and have provided the first vibrational analysis of the D↦X system. The results support the theoretically expected trend toward smaller R_e, larger D_e, and larger ω_e in the D state than in the B state. In fact the experimental results for XeF and XeCl indicate that the differences in the B and D states are even greater than predicted theoretically. The recently demonstrated improved performance of XeCl in a discharge laser seems likely to inspire renewed interest in this laser. Our work should be valuable to such studies. A preprint of the XeCl paper is appended to this report.

Bound-free B↦X emission spectra have been studied as a function of diluent gas pressure for KrCl, ArCl, KrF, and ArF. The most detailed work has so far been done on KrCl, and an analysis of this molecule's spectrum and its vibrational population distribution as a function of pressure (50-800 torr) is nearing completion. Our preliminary estimate of the B-state vibrational frequency is 215 $\pm$ 8 cm^{-1}, which falls right in line with trends indicated in results for other AX molecules we have studied. Our results also indicate that the dipole strength function varies less rapidly with internuclear distance than suggested by theoretical calculations on the AF and XeX systems. This means that while the radiative decay rate of the B-state levels decreases with increasing v, the decrease is not as rapid as suggested by theory. In ArF* and ArCl* the B↦X spectral features seem less sensitive to changes in pressure, suggesting that these excited molecules are initially prepared in lower v levels than are KrCl*(B) and KrF*(B).

We expect to complete all of our work on the rare gas halide spectra, except our study of XeF, during the current contract period. In addition to the work already in progress and outlined above, we intend to reanalyze the XeBr and XeI B↦X systems and look for the KrBr, ArBr, KrI, and ArI B↦X emissions. The last three of these have not previously been observed unambiguously, presumably because they undergo predissociation. However, it is conceivable that the lowest v' levels of these states do not predissociate. In that case it may be possible to observe them at the high pressures (1 atm) employed in our source, where mechanisms other than the bimolecular A* + BX harpooning reactions might produce low v' levels directly (i.e, without extensive vibrational relaxation). In any event we intend to publish the available results in several papers, including a review work on the spectroscopy of these molecules.

B. Halogens

We have succeeded in rotationally analyzing five bands in the UV laser system D'→A' of $^{79}Br_2$, from which we have determined that the A'-state internuclear distance is 2.69 Å. This value is close to the known values for the B(0^+u $^3\Pi$) and A($1u$ $^3\Pi$) states. The rotational analysis corroborates our preliminary vibrational reassignment of this transition. Work continues on this system, with particular emphasis on obtaining and analyzing spectra of $^{81}Br_2$. This work will comprise a major portion of Miss Abha Sur's thesis and should be completed before the end of the present contract period (Feb. 28, 1979).

The full report of the corresponding system in I_2 has not yet been completed but should be ready for submission before the end of the current period. In the meantime the "E→B" system of Cl_2 (2600 Å), which has just recently been made to lase for the first time, continues to resist out attempts to analyze it. However, we are fairly certain that this transition does <u>not</u> terminate on the B state, as presently assumed by most workers. The latter state is now moderately well known and does not appear to be involved in the intense bands in this system.

The proposed studies on the kinetics of A'-state production and removal in the halogens have not yet been initiated, partly for want of equipment (on order from venders), and partly because of waning interest in the laser community. For the latter reason the studies of the pressure dependence of the I_2 UV emission spectrum have also been placed in limbo. Some of this work, including the lifetime determination of the I_2 D' state, we do expect to complete in the present period.

III. Personnel

The Principal Investigator, J. Tellinghuisen, has been occupied with work on this project 30% of academic year time and 100% of summer time. Drs. A. K.

Hui and M. R. McKeever have been employed as Research Associates, Dr. Hui full time, and Dr. McKeever 4/9 time until May 31, 1978 and full time since then. P. C. Tellinghuisen has been employed roughly 1/8 time as Research Associate. Abha Sur continues to devote 100% of research time to this work, in her capacity as Graduate Research Assistant.

IV. Cumulative Listing of Publications and Presentations

1. "Pressure Dependence of the KrF B↦X Spectrum," by Amit K. Hui and Joel Tellinghuisen, contributed talk presented June 17, 1977 at the 32nd Symposium on Molecular Spectroscopy (Ohio State University, Columbus, Ohio).

2. "Intensity Factors for the I_2 B↔X Band System," by Joel Tellinghuisen, J. Quant. Spectrosc. Radiat. Transfer 19, 149 (1978).

3. "Spectroscopic studies of diatomic noble gas halides. III. Analysis of XeF 3500 Å band system," by Joel Tellinghuisen, Patricia C. Tellinghuisen, G. C. Tisone, J. M. Hoffman, and A. K. Hays, J. Chem. Phys. 68, 5177 (1978).

4. "Spectroscopic studies of diatomic noble gas halides. IV. Vibrational and rotational constants for the X, B, and D states of XeF," by Patricia C. Tellinghuisen, Joel Tellinghuisen, J. C. Coxon, J. E. Velazco, and D. W. Setser, J. Chem. Phys. 68, 5187 (1978).

5. "Analysis of the UV Laser Transition in Br_2," by Abha Sur and Joel Tellinghuisen, contributed talk presented June 14, 1978 at the 33rd Symposium on Molecular Spectroscopy (Ohio State University, Columbus, Ohio).

6. "The B↦X and D↦X Systems of XeCl," by Amit K. Hui, Abha Sur, and Joel Tellinghuisen, contributed talk presented June 14, 1978 at the 33rd Symposium on Molecular Spectroscopy (Ohio State University, Columbus, Ohio).

7. "The B↦X System of KrCl," by Mark R. McKeever, Joel Tellinghuisen, and Michael B. Moeller, contributed talk presented June 14, 1978 at the 33rd Symposium on Molecular Spectroscopy (Ohio State University, Columbus, Ohio).

8. "Noble Gas Halides V. The B↦X and D↦X Systems of $^{136}Xe^{35}Cl$," by Abha Sur, Amit K. Hui, and Joel Tellinghuisen, J. Mol. Spectrosc. (submitted).

Noble Gas Halides V. The B+X and D+X Systems of $^{136}Xe^{35}Cl$.

by

Abha Sur, Amit K. Hui, and Joel Tellinghuisen
Department of Chemistry
Vanderbilt University
Nashville, Tennessee 37235

ABSTRACT

The B+X (2870-3100 Å) and D+X (2250-2370 Å) band systems of $^{136}Xe^{35}Cl$ are photographed and vibrationally analyzed. A simultaneous least-squares fit of 41 band heads in the B-X system and 35 in D-X yields, in part, the following constants (in cm^{-1}): T_{eB} = 32405.8, T_{eD} = 42347.9, ω_{eB} = 194.75, ω_{eD} = 204.34, ω_{eX} = 26.22. The ground state dissociation energy (D_e'') is estimated to be 281 ± 10 cm^{-1}. Potential curves are derived for all three states through Franck-Condon calculations. From these curves the D-state internuclear distance is 0.09 ± .02 Å smaller than the B-state distance.

Submitted to the Journal of Molecular Spectroscopy

17 Manuscript pages
6 Figures
6 Tables

SUPPORTED BY ARPA/ONR
UNDER
CONTRACT N00014-76-C-0450

INTRODUCTION

The noble gas monohalide molecules made a big splash three years ago as operating media for a new class of powerful UV lasers (1). XeCl was one of the first of these molecules to be successfully employed in a laser (2), and also the first to be spectroscopically analyzed in any detail (3). Subsequent work has shown that for the transitions of interest only XeCl and XeF display discrete structure in their spectra at the high pressures (~1 atm) characteristic of laser operation. In all other cases transitions from low v' levels of the ionic B(1/2) and D(1/2) states terminate in the vibrational continuum of the $X\ ^2\Sigma^+$ ground state, hence are bound-free (4).[1]

Recent work has provided a detailed description of both discrete transitions, B+X and D+X, in XeF (5-8). One interesting result of these studies is that the D state has a larger D_e, a larger ω_e, and a smaller R_e than does the B state (7). This relationship is predicted qualitatively by theoretical considerations and detailed calculations (9) and is expected to hold in most if not all of the rare gas monohalide species.

The previous analysis of the XeCl emission spectrum (3) treated only the vibrational structure in the lasing or B+X system near 3080 Å and spanned only the lowest 7 v' levels and the lowest 8 v" levels. The D+X system has since been observed in low resolution near 2360 Å but has not been analyzed (10,11). It occurred to us that, with its anticipated smaller R_e value, the D state should "sample" higher v" levels in its emission to X. This point is illustrated in Fig. 1, which in fact summarizes the results of our present study. Both systems terminate on the repulsive wall of the X state, hence display only violet-degraded bands. We find that the strong v" progression for v_D = 0 can be followed to v" = 11, which is 5 levels higher than seen for v_B = 0. The v' progressions connecting

with v" = 0 are recorded up to v_D = 9 and v_B = 12. By using single isotopes of Xe and Cl, we obtain spectra with much sharper heads and are able to identify additional weak B→X bands which were previously obscured by isotopic blending. The latter assignments extend the X-state observations to v" = 13, which is only 15 cm^{-1} below dissociation. A weighted least-squares fit of all assigned B→X and D→X bands gives a significantly improved description of the vibrational level structure in the X, B, and D states. Trial-and-error Franck-Condon calculations then lead to the potential curves of Fig. 1, which are considered reliable in a relative sense.

EXPERIMENTAL

The XeCl emission was produced by a mild high-frequency discharge of $^{136}Xe/^{35}Cl_2$/Ar mixtures containing about 2.5 torr ^{136}Xe, 1.5 torr $^{35}Cl_2$, and 200-600 torr Ar. Preliminary work had indicated that this approximate composition yielded best intensity for D→X, which was typically 25-50 times weaker than B→X. The ^{136}Xe (isotopic purity 95.16%) was obtained from Mound Laboratory of Monsanto Research Corporation. The ^{35}Cl was procured from Oak Ridge in the form of $Na^{35}Cl$ (isotopic purity 99.35%). Chlorine vapor was produced from this by reaction with dry CrO_3. The two reagents were first dried separately, then mixed and warmed with a heat gun, all operations being carried out under vacuum. The reaction produces CrO_2Cl_2, which releases Cl_2 on photolysis with visible light.

Spectra were recorded on a J-Y HR 1500 1.5-meter Czerny-Turner spectrometer equipped with a 3600-groove/mm holographic grating. The first-order reciprocal dispersion was 1.49 Å/mm in the 3000 Å region and 1.64 Å/mm near 2300 Å. All spectra were recorded using slit widths of 10 μm or less. The B→X system was photographed on Kodak Ia-O plates using exposures ranging from a few seconds to a few minutes. Kodak SWR film was used to record the D→X system, with exposures as long as 30 minutes required for the high-v' bands. Calibration spectra were obtained from a microwave discharge Fe lamp using exposures of 1-3 s. The plates and films were developed in Kodak D-19 Developer for 4-5 min. and 1-2 min., respectively. The shorter development times for the latter gave significantly fewer of the inevitable scratches and blemishes characteristic of gelatinless films.

The spectra were measured on a Grant comparator. The calibration lines on each exposure (approximate coverage 40 Å) were least-squares fitted to a quadratic or cubic polynomial with standard deviations typically 0.002-0.003 Å. Edlen's formula (12) was used to convert the standard air wavelengths to vacuum wavenumbers. Spectra were taken at grating intervals of less than 20 Å so that every feature would appear on at least two different exposures. All of the strong, distinct band edges were indeed measured at least two and occasionally three times. The spread in the measured frequencies for such features seldom exceeded 0.2 cm^{-1} for B→X and 0.3 cm^{-1} for D→X, which we take as an indication of the reliability of the measurements. A similar figure emerged from the least-squares parameter determination, discussed below.

RESULTS AND DISCUSSION

Figure 2 displays the long-wavelength ends of both band systems. Once the measurements were in hand, the band assignments were a straightforward extension of the previous work (3). There were no measured heads that could not be assigned. The B→X system is essentially as described earlier, except, as noted above, considerably cleaner without isotopic blending. The v'-v" intensity pattern in the D→X system is similar to that for B→X, except displaced to higher v" levels in agreement with the anticipated smaller R_e value in the D state. Thus, for example, in the B→X system the v' = 0 progression shows peak intensity near v" = 1 and 2 and vanishes beyond v" = 6. In D→X this progression attains peak intensity for v" = 3

and 4 is observed to v" = 11; moreover the 0-0 band is only barely discernible. The intensity patterns of both systems are generally well reproduced in the Franck-Condon calculations described below.

Although rotational structure is partially resolved in some bands, we have made no attempt to analyze it. The branch structure is expected to be similar to that in XeF (6), where four distinct branches stem from the mixed coupling situation, with strong Hund's case c character in the B and D states. The XeCl spectrum is much more congested than the XeF spectrum because of the smaller rotational constant and especially the very small vibrational spacing in the X state. For our present resolution a successful rotational analysis appears unlikely. However we have calculated typical band structures by estimating the splitting constants and rotational constants as described in Ref. (6), and have confirmed that for the potential curves deduced here (Fig. 1) the only heads occur in the P branches less than 1 cm^{-1} to the red of the origin in B-X and within 1.6 cm^{-1} of the origin in D-X. Synthetic band profiles for the 0-0 and (hypothetical) 0-12 bands of B+X are illustrated in Fig. 3. Note that while both bands show a single long-wavelength edge, the lines of the latter spread out to the blue more rapidly (because of the smaller B" value), and consequently the head is much less prominent. Furthermore the high-v" bands break off into diffuse emission at fairly low N, as the lower level becomes rotationally unbound. These effects make the high-v" bands (e.g. 2-11, 2-12, 2-13 in B-X) difficult to discern in the spectrum, even though Franck-Condon factors (FCFs) are favorable (see below). The bands of the D+X system are similar in appearance to those shown in Fig. 3. In both systems the magnitude of the origin-head spacing decreases as $B_{v''}$ decreases (v" increases), so there will be slight systematic errors in vibrational parameters determined from the band heads. However, lacking more detailed information about the rotational structure in XeCl, we consider that head + origin corrections, which were important in the XeF

analysis (7), are not warranted here. The main consequence of their neglect is that our T_e values are likely to be too low by ~0.8 cm^{-1} for the B state and ~1.6 cm^{-1} for the D state.

Wavelengths and wavenumbers of the assigned bands are listed in Tables I and II together with weights and deviations from the least-squares fit. The weights were assessed to reflect at least semiquantitatively the precision of the measurements and ranged from 1 to 5 for B-X bands and 1 to 3 for D-X. There were in addition several weak bands (including 2-11, 2-12, and 2-13 in B-X) which were estimated from photographic enlargements of the spectra; these were given weights of 0.5. Vibrational parameters were obtained from a simultaneous fit of both systems, as was used for XeF (7). The number of parameters was varied from 2 to 3 for the B and D states and 3 to 6 for the X state, with absolute minimum variance obtained for the (3,3,6) fit. However, all fits employing more than 8 vibrational parameters gave at best only 17% lower variance than the more compact (2,2,4) fit. Since the constants from the latter were better behaved (for the purpose of extrapolation to levels beyond the observations) than those from higher order fits, we recommend them as the best condensation of our measurements. The values are presented in Table III together with related information discussed below. The vibrational parameters have their usual significance as coefficients in polynomials in $(v + \frac{1}{2})$, e.g.,

$$G_{v''} = \sum_{i=1}^{4} c_{vi}''(v'' + \tfrac{1}{2})^i \quad . \qquad (1)$$

The vibrational constants in Table III are in general accord with the previous results for the B and X states but are far more precise. Note that $\omega_e x_e$ is again a negative number for the X state; nonetheless, $\Delta G''_{v+\frac{1}{2}}$ declines monotonically with v", as before. The vibrational frequency in the D state is higher than in B, but the increase is much smaller than observed in XeF (7) - 5% vs 13%. This result is

consistent with the expectation of weaker configuration interaction between the zero-order $^2\Gamma^+$ states in XeCl, which are energetically further apart than in XeF. Both ω_e values in XeCl are greater than the theoretical estimates (188 and 189 cm^{-1}) of Hay and Dunning (9) but less than the ground state frequency of $^{133}Cs^{35}Cl$ (214.22 cm^{-1}). The same comparison for XeF yields similar results, except that the XeF D state frequency is very close to the $^{133}Cs^{19}F$ ground state frequency (350.14 vs 352.56 cm^{-1}).

To estimate the dissociation energy of the ground state, we employ long range theory (12) as before (3,7). The quantities G_v and g in the relationship

$$g(G_v) \equiv (dG_v/dv)^{3/2} = K_6^{3/2}(\mathcal{D}_e - G_v) \quad , \qquad (2)$$

and their error band are calculated from the four X state parameters in Table III and their variance-covariance submatrix. For the highest observed levels in the X state, the plot of Eq. (2) is approaching the predicted linear behavior (Fig. 4). A short extrapolation having the theoretical slope, $-K_6^{3/2}$, yields $\mathcal{D}_e = 281\ cm^{-1}$. Here K_6 is related to the reduced mass and the R^{-6} potential coefficient by (12)

$$K_6 = 59.83/[\mu^{1/2}(c_6)^{1/6}] \qquad (3)$$

(units amu, cm^{-1}, and Å), and as before, we employ a theoretical estimate of $c_6 = 8 \times 10^5\ cm^{-1}\ Å^6$ to calculate the limiting slope, $-K_6^{3/2} = -1.278$. Using the expression (12)

$$[(v_D - v)(K_6/3)]^3 = \mathcal{D}_e - G_v \qquad (4)$$

we obtain $v_D = 19.26$, indicating that there are 20 bound levels in the X state. The error band on the solid curve in Fig. 4 is very narrow and gives a precision of ~3 cm^{-1} for $\mathcal{D}_e$. For a more conservative and probably more realistic error estimate we examine the results from the 5- and 6-parameter fits for the X state.

The latter agree well with the 4-parameter results, but in the former case the g vs G_v curve flares up before attaining the theoretical slope. An extrapolation of the linear region (Fig. 4) yields $\mathcal{D}_e = 291\ cm^{-1}$. On the other hand preliminary results obtained before the 2-11, 2-12, and 2-13 bands of B-X were assigned yielded an estimate of 271 cm^{-1}. From these considerations we think it likely that the true value is within 10 cm^{-1} of 281 cm^{-1}. This estimate is 26 cm^{-1} larger than the previous value (3), which was based on an extrapolation of data coverying only the first 8 v" levels.

The $\mathcal{D}_e$ values for dissociation of the B and D states to ions are calculated from the known Xe ionization potentials (97834 and 108372 cm^{-1}) (13) and the Cl electron affinity (3.615 eV) (14), together with the T_e and $\mathcal{D}_e$" values. The results (Table III) show that the D state is deeper than the B state in XeCl, just as in XeF. However, as in the ω_e comparison, the difference is smaller in XeCl.

Without a rotational analysis we cannot determine absolute potential curves for the three states. However, we are able to deduce the approximate relative configuration of Fig. 1 by comparing the observed intensity patterns with FCFs computed in trial-and-error fashion for various curve shapes and internuclear separations. As in previous work on these molecules, we assume that the B and D curves can be adequately represented by a truncated Rittner potential (15)

$$U(R) = a + b\exp(-\beta R) - c_1/R - c_3/R^3 - c_4/R^4 \quad , \qquad (5)$$

in which all constants except b, β, and R_e are fixed at the outset. The latter are then determined by the experimental $\mathcal{D}_e$ and ω_e values. The ion-induced dipole coefficient c_4 is as given before (3). The ion-quadrapole term, $-c_3/R^3$, was discussed in Ref. (4) but was omitted from the potentials employed there. It is included here, because its presence leads to better agreement with the experimental R_e for

the B state of XeF.[2] The c_3 value for the B state is estimated from (4)

$$c_3 = (e^2/5)\langle r^2\rangle \quad . \qquad (6)$$

Here $\langle r^2\rangle$ is the average r^2 value for the valence p electrons in the $Xe^+ \ ^2P_{3/2}$ ion. Using the non-relativistic $\langle r^2\rangle$ value for Xe (16) and Slater's rules to estimate the percent decrease on ionization, we obtain 1.66 $Å^2$ and thence the c_3 value in Table III. For the D state, which correlates with the quadrupoleless $^2P_{\frac{1}{2}}$ state of Xe^+, $c_3 = 0$. The quantity a in Eq. (5) is simply the asymptotic ionic energy relative to the X state minimum.

The values of b, β, and R_e obtained for the B and D states of XeCl are included in Table III. These Rittner curves predict $\omega_e x_e$ values of 0.642 cm^{-1} for B and 0.716 for D, both in good agreement with experiment. In fact for all our observed levels the quantum mechanical eigenvalues of these potentials agree with the experimental G_v values within 0.5 cm^{-1} for the B state and 2.1 cm^{-1} for D.

For the X curve we started with the repulsive branch determined previously, but shifted 0.07 Å to larger R in keeping with the larger R_e value of the present B state. The upper portion of the curve was varied in systematic fashion while the region below v" = 6 was held fixed to preserve the previous agreement in the FCFs for these levels. For each repulsive branch the attractive branch was adjusted to give the correct RKR turning point differences, $R_{max} - R_{min}$, which depend on the vibrational constants alone. For each of the several trial curve shapes, FCFs were computed over a range of internuclear separations for both band systems. Using the B state Rittner curve as the fixed reference, we obtained best agreement with an X curve having a repulsive branch representable as a Morse curve through the three points, U(3.25 Å) = 0, U(3.03) = 22 cm^{-1}, U(2.83) = 200 cm^{-1}. This curve was extended to smaller R by an R^{-12} form attached at R = 2.81 and 2.83 Å.

With the B and X curves thus determined, the Rittner potential for the D state was found to reproduce the observed D→X intensity pattern without any further adjustment of R_{eD}.

The final X curve (Table IV) differs in shape only slightly from the previous determination, in the region of importance for our spectra (2.7-3.2 Å). However, as R decreases to 2 Å, the present R^{-12} extension rises much more slowly than the previously used exponential form. The new extension is more reasonable, as has been verified in simulations of the low-pressure bound-free emission spectrum (17). Relative to either the B or the D curve, our X curve should be reliable within 0.015 Å in the 2.8-3.1 Å region.

We reiterate that the potential curves of Fig. 1 and Tables III and IV are valid only in the relative sense, as we have not analyzed rotational structure. The *ab initio* R_e's of Hay and Dunning (9) are 3.22 Å for B and 3.18 Å for D, or about 0.25 Å greater than the Rittner model predictions. The theoretical calculations underestimate the difference in the B and D state R_e's of XeCl by a factor of two. A similar discrepancy occurs in the XeF calculations (9), where absolute R_e's are known experimentally. In the latter molecule the Rittner model underestimates the B- and D-state R_e's by 0.06 Å and 0.01 Å, respectively, while the theoretical calculations overestimate by 0.05 Å and 0.11 Å, respectively. From such comparisons it seems likely that the true R_e's in XeCl are bracketed by the Rittner model predictions and the *ab initio* results. This conclusion is compatible with results for the ground state from scattering experiments (18).

The final FCFs for the first 6 v' levels of each system are given in Tables V and VI. Included are results for rotationless curves and for N' = N" = 50, which corresponds roughly to the average value in the excited states at T = 325 K (the estimated temperature of our source).[3] Here as in XeF (7) there is a significant

rotational dependence in the FCFs and a tendency for the intensities to be wavelength rather than quantum number dependent. This point is illustrated in Fig. 5, where the FCFs for the $v' = 0$ progression in the B-X system are plotted as a function of wavelength, for $N = 0$ and 50. (This figure also serves to illustrate the overlap problem, which makes the rotational structure so complex.) Note that the rotationless FCFs are the appropriate quantities for our potential curve determination, because we are concerned with the intensities near the band heads, which occur at $N' < 12$ in both systems.

The comparison of Fig. 5 is more informative when the quantity plotted is the Franck-Condon density (FCD) instead of the FCF. Because the density of v'' levels for $N' = 50$ is greater than for $N'' = 0$, the FCD for the discrete spectrum, defined as

$$FCD(v' \rightarrow v'') = FCF(v',v'')/(dG_{v''}/dv'') \quad , \qquad (7)$$

is comparable for the two N'' values, as shown in Fig. 6. The discrete FCD of Eq. (7) extrapolates smoothly to the true bound-free FCD at the wavelength corresponding to the dissociation limit (19,20). Bound-free emission is important for all levels above $v' = 0$ in these XeCl transitions, as is evident from the curves for $v' = 1$ and 2 in Fig. 6. The structure in these curves is similar to that which occurs in the bound-free B→X systems of other rare gas halides, as may be seen in the decomposed XeBr spectrum given earlier (4). However, because the X curve of XeCl is flatter in the Franck-Condon region, the interference-type character (20) associated with the minimum in the difference potential, $V(R) = U_B(R) - U_X(R)$, is already apparent in the emission from $v' = 2$. In other words the curves in Fig. 6 display more peaks than expected from the reflection principle, whereas the structure in the bound-free B→X spectra of XeBr, XeI, KrF, KrCl, ArF, and ArCl is more

correctly described as reflection structure. In all these transitions the emission from low v' levels ends on the repulsive wall of the X state, but in XeCl the relevant segment of the X curve is flatter and lies to a large extent within the ground state well.

CONCLUSION

Using sources containing isotopically pure ^{136}Xe and $^{35}Cl_2$, we have photographed and vibrationally analyzed the B→X and D→X systems of $^{136}Xe^{35}Cl$. A simultaneous least-squares fit of both systems gives improved constants for the B and X states and the first description of the D state. These constants may be used with the appropriate isotopic ρ factors to calculate frequencies for other isotopic molecules occurring in "natural" XeCl sources. On comparing the heaviest and lightest isotopomers of significance ($^{136}Xe^{37}Cl$ and $^{129}Xe^{35}Cl$), we find the shifts to be appreciable even for the $v' = 0$ progressions (2.3 cm^{-1} for the 0-0 bands). Thus the XeCl laser may be viewed as operating on a semicontinuum of overlapped rotational lines of some 10 isotopic molecules. It is conceivable that its operating characteristics would be significantly different with a single XeCl species.

With the completion of this analysis, the strong systems, B-X and D-X, in two members of the "new" noble gas monohalide class - XeF and XeCl - may be regarded as reasonably well understood. Rotational structure has not yet been analyzed in XeCl, but is expected to resemble that in XeF. Our results verify an anticipated trend toward smaller R_e, larger ω_e, and larger $\mathcal{D}_e$ in the D state as compared with the B state. The C(3/2) state, which is estimated to lie near or slightly below the B state, is not manifested in our spectra in any way. Thus this state remains spectroscopically ill-defined in all the rare gas halide molecules.

REFERENCES

1. J. J. Ewing, Physics Today, Vol. 31, No. 5, 32 (May, 1978).
2. J. J. Ewing and C. A. Brau, Appl. Phys. Lett. 27, 350 (1975).
3. J. Tellinghuisen, J. M. Hoffman, G. C. Tisone and A. K. Hays, J. Chem. Phys. 64, 2484 (1976).
4. J. Tellinghuisen, A. K. Hays, J. M. Hoffman and G. C. Tisone, J. Chem. Phys. 65, 4473 (1976).
5. A. L. Smith and P. C. Kobrinsky, J. Mol. Spectrosc. 69, 1 (1978).
6. J. Tellinghuisen, P. C. Tellinghuisen, G. C. Tisone, J. M. Hoffman and A. K. Hays, J. Chem. Phys. (in press).
7. P. C. Tellinghuisen, J. Tellinghuisen, J. A. Coxon, J. E. Velazco and D. W. Setser, J. Chem. Phys. (in press).
8. D. L. Monts, L. M. Ziurys, S. M. Beck, M. G. Liverman and R. E. Smalley (to be published).
9. P. J. Hay and T. H. Dunning, Jr., J. Chem. Phys. (in press).
10. J. E. Velazco, J. H. Kolts and D. W. Setser, J. Chem. Phys. 65, 3468 (1976).
11. R. Shuker, Appl. Phys. Lett. 29, 785 (1976).
12. R. J. LeRoy, Specialist Periodical Report on Electronic Spectroscopy, Chemical Society (London), edited by R. F. Barrow, Vol. 1, p. 113 (1973).
13. C. E. Moore, U. S. Natl. Bur. Stand. Circ. 467, Vol. III (1958).
14. M. Hotop and W. C. Lineberger, J. Phys. Chem. Ref. Data 4, 539 (1975).
15. P. Brumer and M. Karplus, J. Chem. Phys. 58, 3903 (1973).
16. J. P. Desclaux, At. Data and Nuc. Data Tables 12, 312 (1973).
17. K. Tamagake and D. W. Setser, J. Chem. Phys. (to be published).
18. C. Becker, P. Casavecchia, J. Valentini and Y. T. Lee, (to be published).
19. J. Tellinghuisen, J. Chem. Phys. 59, 849 (1973).
20. J. Tellinghuisen, in États Atomiques et Moleculaires Couplés a un Continuum. Atomes et Molécules Hautement Excités, p. 317, Centre National de la Recherche Scientifique, Paris (1977).

FOOTNOTES

1. The labeling of the states here is the same as employed in Ref. (4).
2. In the present application, the main effect of adding the attractive R^{-3} term is an increase in R_e.
3. The FCFs were calculated for the hypothetical Q branch transitions, with both states treated as Hund's case b. In other words the same centrifugal term $\propto N(N+1)/R^2$ was added to both states. This procedure is customary and is entirely adequate within the context of the present study.

FIGURE CAPTIONS

Fig. 1 - Potential diagram for XeCl, showing the states of relevance to the present study. Note the different energy scales for the three potential curves.

Fig. 2 - The long-wavelength regions of the B→X and D→X emission spectra of $^{136}Xe^{35}Cl$, with vibrational assignments indicated.

Fig. 3 - Synthetic band profiles for 0-0 and 0-12 bands of XeCl B→X system, computed using the methods of Ref. (6) and the following constants (cm^{-1}): B_0' = 0.0669, B_0'' = 0.0560, B_{12}'' = 0.0274, D_0' = 3.2 x 10^{-8}, D_0'' = 9.3 x 10^{-7}, D_{12}'' = 1.9 x 10^{-6}, H_0'' = -2 x 10^{-11}, H_{12}'' = -1.8 x 10^{-10}, λ_0 = 3077.0 Å, δ = 2.0, α = -0.4, T = 325 K, Resolution = 0.1 Å.

Fig. 4 - g (units $cm^{-3/2}$) vs G_v and v for the X state of XeCl. Solid curve - from results of (2,2,4) fit; broken curve - from results of (3,3,5) fit.

Fig. 5 - Franck-Condon factors for bands in the v' = 0 progression of the XeCl B-X system, plotted vs wavelength. Solid lines - N' = N'' = 0; broken lines - N' = N'' = 50.

Fig. 6 - Franck-Condon density for v' = 0, 1, and 2 of the B→X system, plotted vs wavelength. Solid curves and filled points - N' = N'' = 0; borken curves and open points - N' = N'' = 50. Points on curves were calculated using Eq. (7). Wavelengths corresponding to emission to the dissociation limit of the X state are indicated at the top for each v' and N, e.g. $D_{1,0}$ delimits the discrete emission (to the blue) and diffuse emission (to the red) from v' = 1, N' = 0.

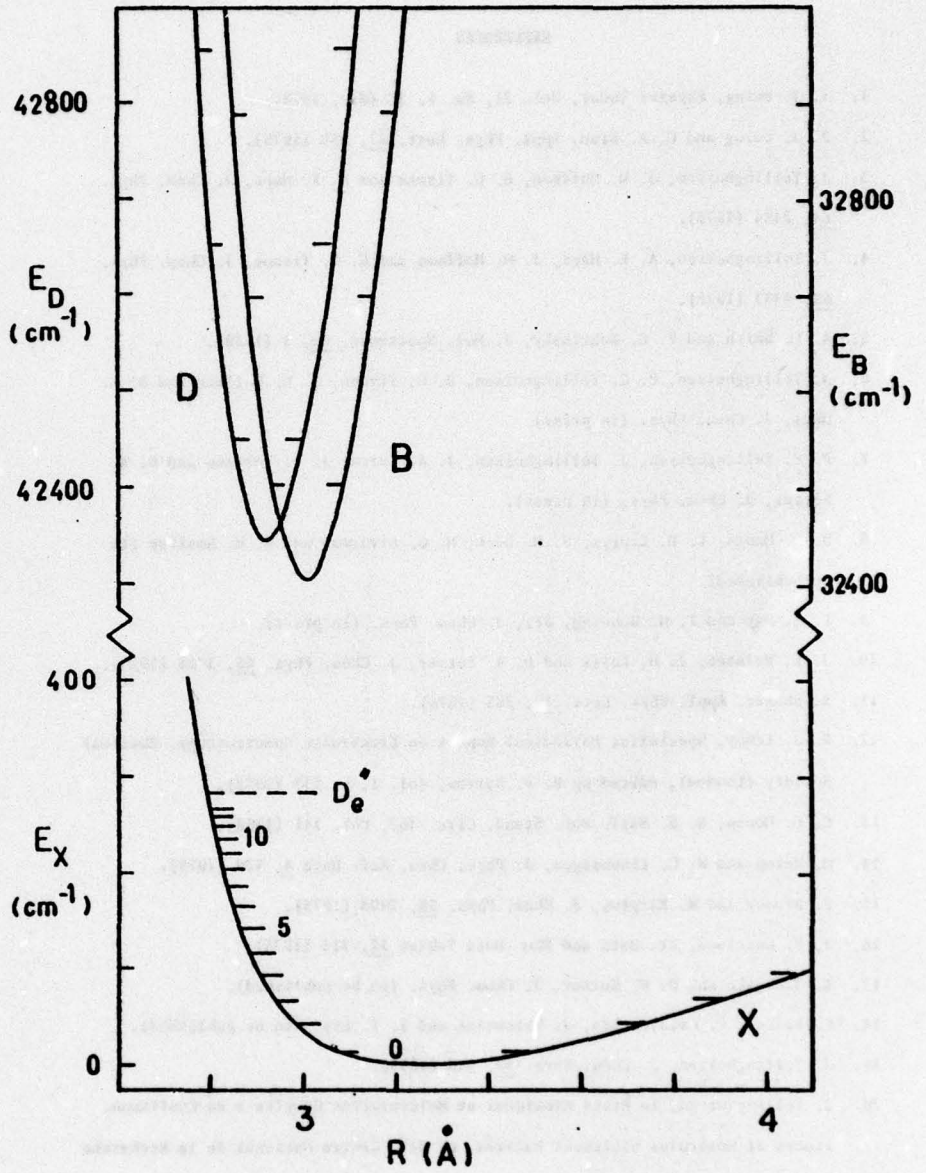

Fig. 1 - Sur, et al., J. Mol. Spectrosc.

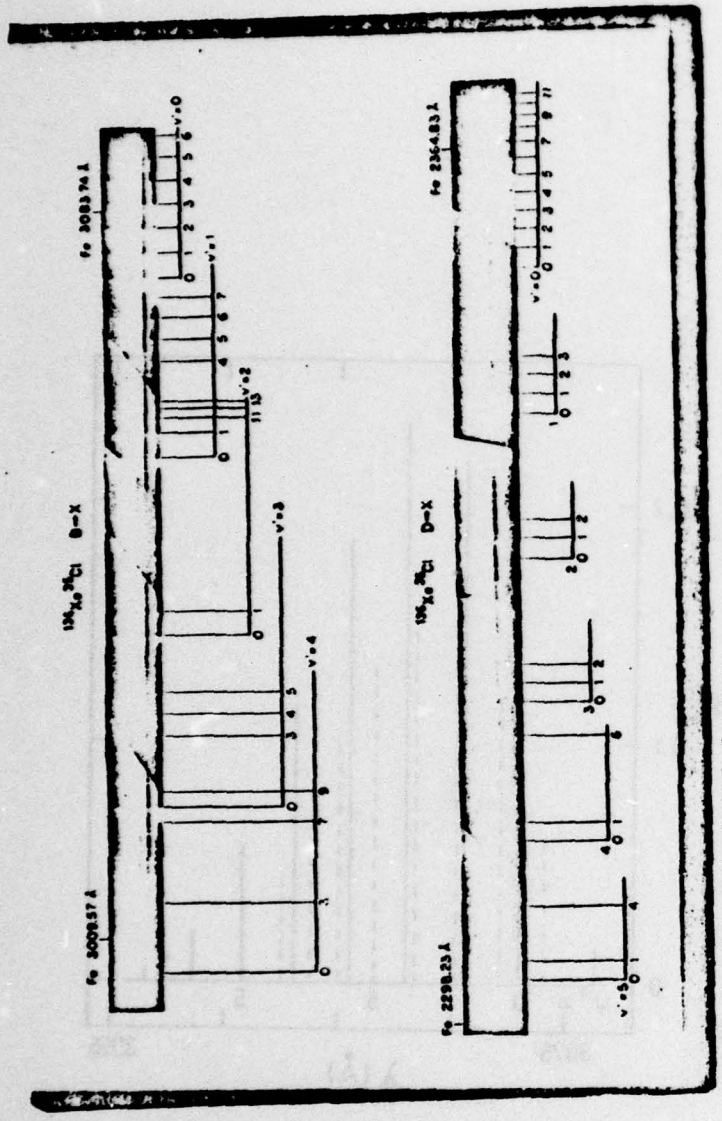

Fig. 2 - Sur, et al., J. Mol. Spectrosc.

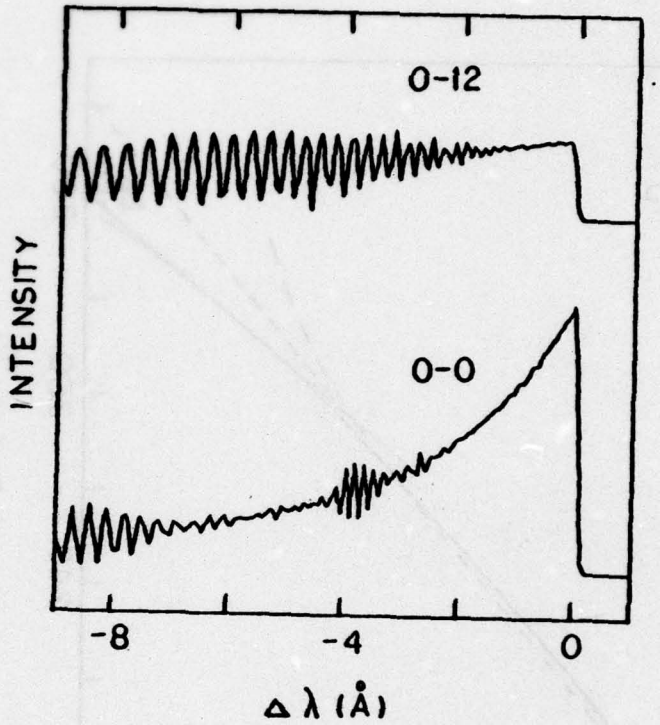

Fig. 3 - Sur, et al., J. Mol. Spectrosc.

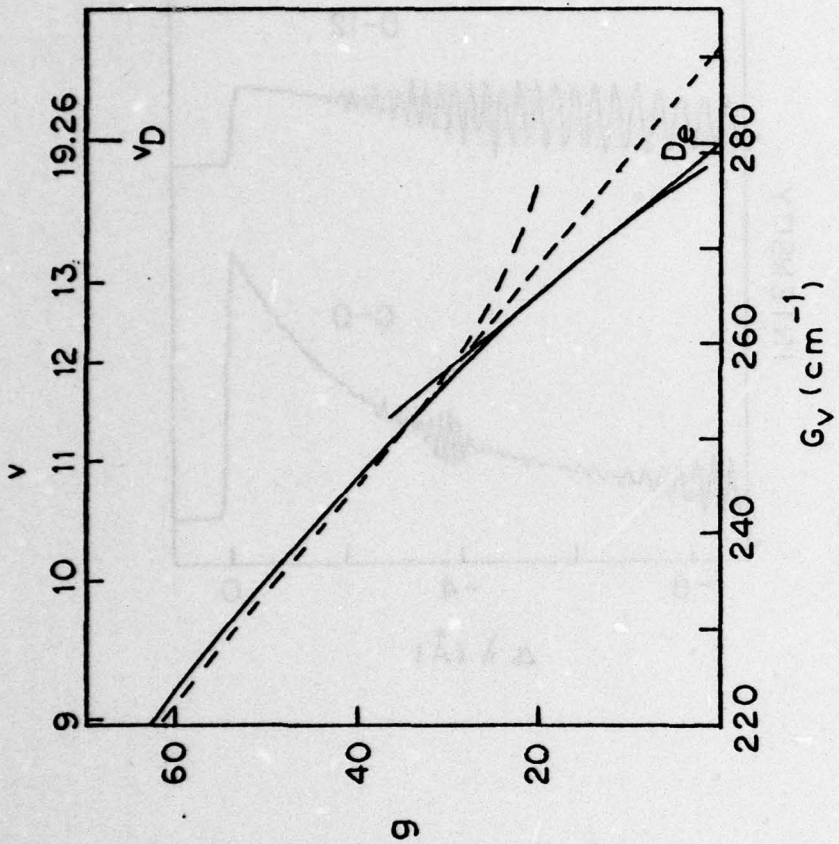

Fig. 4 - Sun, et al., J. Mol. Spectrosc.

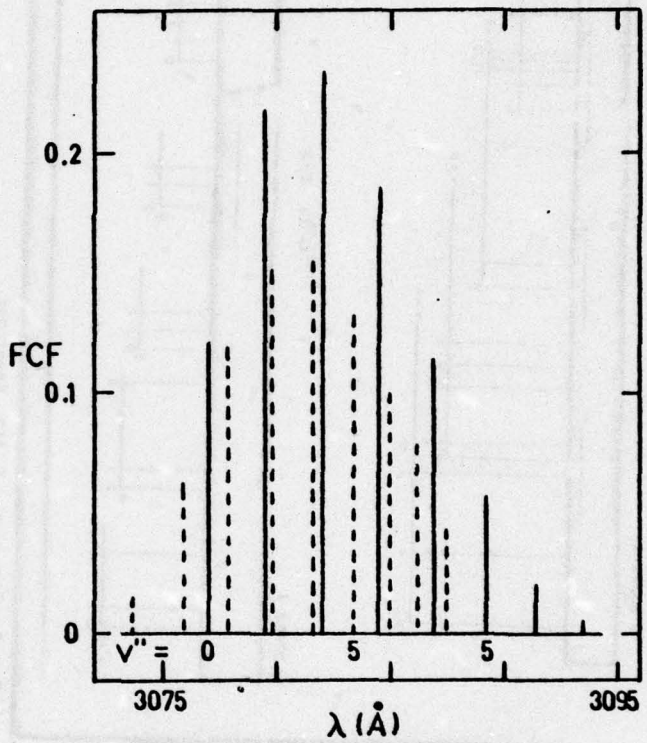

Fig. 5 - Sun, et al., J. Mol. Spectrosc.

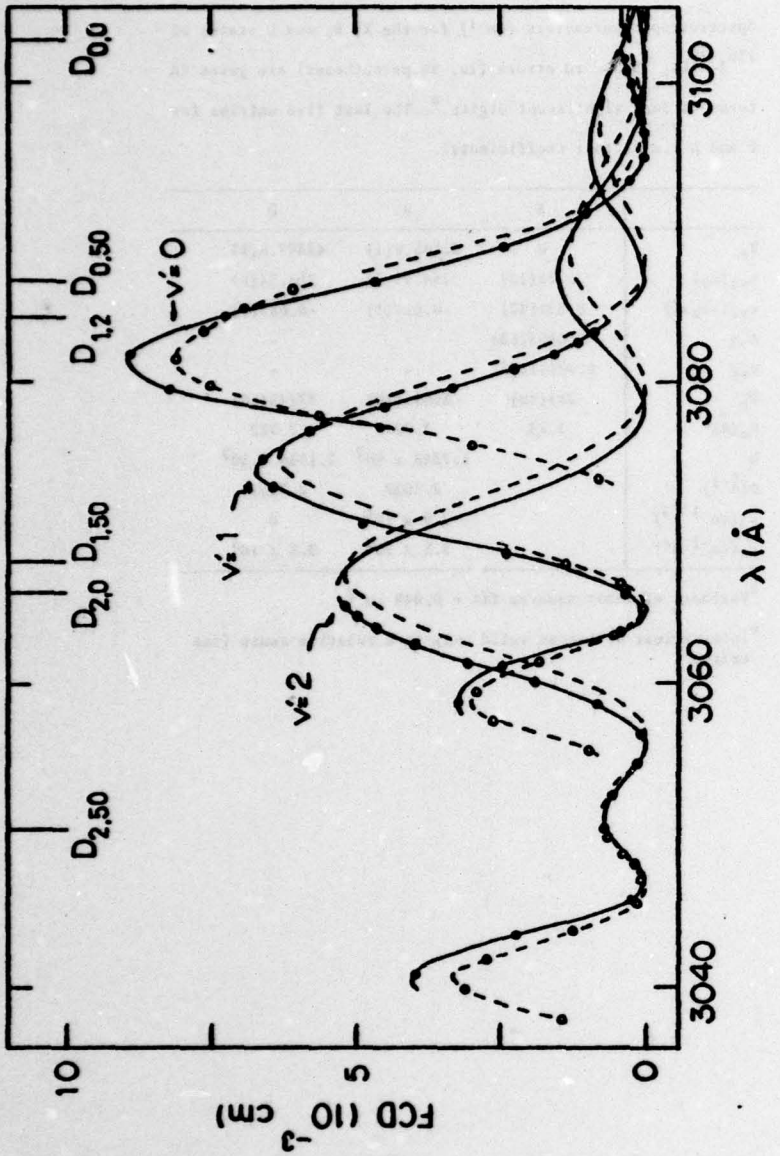

Fig. 6 - Sur, et al., J. Mol. Spectrosc.

TABLE I

Assigned Band Heads in B→X Spectrum of $^{136}Xe^{35}Cl$

v'-v"	Height	λ(Å)	ν(cm^{-1})	Δν(cm^{-1})[a]
0-6	1	3091.37	32338.7	0.3
0-5	1	89.21	361.3	0.2
0-4	5	86.90	385.6	-0.0
0-3	5	84.50	410.8	-0.1
0-2	5	82.04	436.7	0.1
0-1	5	79.53	463.0	0.3
0-0	5	76.98	490.0	-0.1
1-7	3	74.91	511.8	-0.0
1-6	3	72.97	532.4	0.2
1-5	5	70.83	555.1	0.0
1-4	5	68.55	579.3	-0.2
2-13	0.5	64.46	622.7	0.1
2-12	0.5	63.75	630.2	0.7
2-11	0.5	62.76	640.8	0.4
1-1	5	61.26	656.8	-0.0
1-0	5	58.75	683.6	-0.2
2-1	5	43.35	849.0	0.0
2-0	5	40.89	875.6	0.0
3-5	0.5	35.17	937.5	0.8
3-4	2	32.91	962.1	0.2
3-3	5	30.55	987.7	-0.2
3-1	0.5	25.80	33039.5	0.5
4-9	0.5	24.97	048.5	0.5
3-0	5	23.30	066.8	-0.2
4-7	0.5	21.68	084.5	0.2
4-3	0.5	13.26	177.0	0.2
4-0	5	06.07	256.4	-0.0
5-3	5	2996.21	365.8	-0.1
5-2	3	93.87	391.8	-0.1
5-0	3	89.11	445.0	-0.2
6-0	5	72.48	632.1	-0.1
7-2	5	60.80	764.9	0.1
7-0	3	56.15	817.9	0.2
8-0	5	40.09	34002.7	0.1
9-0	5	24.31	186.1	0.1
10-1	5	11.06	341.7	0.1
10-0	5	08.80	368.4	0.1
11-1	5	2895.78	522.9	-0.1
11-0	5	93.55	549.5	-0.1
12-1	2	80.76	702.9	-0.4
12-0	2	78.60	728.9	0.2

[a] $\nu_{calc} - \nu_{obs}$, from least-squares fit.

TABLE II

Assigned Band Heads in D→X Spectrum of $^{136}Xe^{35}Cl$

v'-v''	Height	λ(Å)	ν(cm^{-1})	Δν(cm^{-1})[a]
0-11	0.5	2368.74	42203.7	-1.4
0-10	1	68.07	215.5	-0.8
0-9	2	67.31	229.2	0.2
0-8	2	66.35	246.3	-0.1
0-7	3	65.30	264.9	0.2
0-6	3	64.13	285.9	0.0
0-5	3	62.87	308.5	-0.1
0-4	3	61.54	332.3	0.0
0-3	2	60.15	357.3	0.2
0-2	3	58.69	383.4	0.2
0-1	1	57.24	409.5	0.6
1-3	1	48.84	561.3	-0.7
1-2	3	47.44	586.6	-0.0
1-1	2	45.99	612.9	0.2
1-0	2	44.52	639.6	0.1
2-2	1	36.40	787.7	0.4
2-1	2	34.92	814.9	-0.2
2-0	3	33.47	841.5	-0.2
3-2	3	25.50	988.3	0.1
3-1	2	24.05	43015.1	-0.1
3-0	2	22.63	041.4	0.2
4-6	3	20.06	089.2	0.4
4-1	3	13.37	213.7	0.1
4-0	3	11.93	240.5	-0.1
5-4	2	06.95	333.9	-0.3
5-1	1	02.86	410.9	0.4
5-0	2	01.41	438.2	-0.3
6-1	1	2292.52	606.7	0.8
6-0	3	91.10	633.8	0.3
7-3	2	85.02	749.8	-0.1
7-0	3	80.90	828.8	0.1
8-0	3	70.88	44022.3	0.0
9-3	2	65.07	135.1	0.1
9-2	1	63.71	161.7	-0.4
9-0	1	61.01	214.4	-0.7

[a] $\nu_{calc} - \nu_{obs}$, from least-squares fit.

TABLE III

Spectroscopic parameters (cm^{-1}) for the X, B, and D states of $^{136}Xe^{35}Cl$. Standard errors (1σ, in parentheses) are given in terms of last significant digits.[a] The last five entries for B and D are Rittner coefficients.

	X	B	D
T_e	0	32405.8(1)	42347.9(1)
$c_{v1}(\omega_e)$	26.22(12)	194.75(3)	204.34(6)
$c_{v2}(-\omega_e x_e)$	0.321(47)	-0.627(3)	-0.682(7)
c_{v3}	-0.0853(63)	-	-
c_{v4}	0.00191(26)	-	-
D_e	281(10)	36553(10)	37148(10)
R_e(Å)[b]	3.23	3.007	2.922
b		1.7348×10^7	2.1316×10^7
β(Å^{-1})		2.5637	2.7261
c_3(cm^{-1} Å^3)		3.9×10^4	0
c_4(cm^{-1} Å^4)		3.5×10^5	3.5×10^5

[a] Variance of least-squares fit = 0.048 cm^{-2}.

[b] Internuclear distances valid only in a relative sense (see text).

TABLE IV

Turning Points for the X $^2\Sigma^+$ Potential Curve of $^{136}Xe^{35}Cl$

v	$G_v(cm^{-1})$	$R_{min}(\mathring{A})$[a]	$R_{max}(\mathring{A})$[a]
-0.5	0.0	R_e = 3.23	
-0.4	2.63	3.1442	3.3363
-0.2	7.89	3.0944	3.4266
0	13.18	3.0645	3.4927
0.2	18.49	3.0422	3.5483
0.6	29.13	3.0091	3.6425
1	39.78	2.9843	3.7235
2	66.31	2.9400	3.8971
3	92.34	2.9089	4.0512
4	117.51	2.8853	4.1991
5	141.49	2.8664	4.3477
6	163.99	2.8511	4.5024
7	184.77	2.8385	4.6680
8	203.65	2.8281	4.8493
9	220.48	2.8195	5.0521
10	235.15	2.8124	5.2839
11	247.63	2.8065	5.5554
12	257.89	2.8019	5.8822
13	265.98	2.7982	6.2906

[a]Four decimal places are retained to minimize interpolation errors.

TABLE V

Franck-Condon Factors (x 10^3) for B-X System of $^{136}Xe^{35}Cl$[a]

v''	v' = 0	1	2	3	4	5
0	121 16	84 20	105 30	93 37	93 44	82 50
1	218 63	65 54	60 66	20 60	8 56	0 45
2	234 119	10 61	6 58	5 31	13 17	32 5
3	186 153	7 37	4 25	43 3	32 0	36 6
4	115 155	58 10	16 3	52 4	14 11	8 23
5	57 133	114 0	12 1	30 19	0 20	1 24
6	21 100	140 6	2 5	8 27	10 16	10 12
7	5 79	131 18	2 8	0 27	28 10	13 5
8	0 44	103 25	14 7	1 17	35 3	7 0
9	0	71	29	2	31	1
10	1	45	41	2	22	0
11	2	26	45	1	14	2
12	2	15	42	0	8	4
13	2	8	35	0	4	5
14	2	4	26	0	2	5

[a]First entry is for N'=N''=0. Second entry, where given, is for N'=N''=50.

TABLE VI

Franck-Condon Factors (x 10^3) for D-X System of $^{136}Xe^{35}Cl$[a]

v''	v' = 0	1	2	3	4	5
0	29	41	56	66	73	77
	3	6	10	15	20	26
1	73	70	74	60	45	29
	13	22	33	41	47	49
2	114	67	48	20	5	0
	31	41	50	50	44	34
3	139	41	15	0	5	17
	52	51	49	35	21	8
4	142	13	0	10	22	30
	69	48	35	15	3	0
5	128	0	4	26	27	20
	78	37	18	2	0	6
6	105	5	14	31	17	6
	77	23	6	0	5	13
7	79	19	18	25	6	0
	76	14	2	2	10	15
8	57	33	17	15	0	2
	55	5	0	5	10	11
9	39	44	12	7	1	6
10	26	47	7	2	4	9
11	17	45	3	0	6	8
12	11	39	1	0	7	7
13	7	31	0	0	6	5
14	4	23	0	0	5	3

[a]First entry is for N'=N''=0. Second entry, where given, is for N'=N''=50.